

Non-Uniform Temperature Distribution Generation of Resistively Heated Reinforced Carbon-Carbon

James A. Brennan¹

University of New South Wales at the Australian Defence Force Academy

Assessment of aircraft that operate within high Mach numbers have indicated that aerodynamic heating encountered within these conditions generates non-uniform temperature profiles along its external surfaces. Finite Element Modeling has been performed to assess the effect of resistive heating on Reinforced Carbon-Carbon with changing cross section has on surface temperature distribution. Changes in cross sectional area of Reinforced Carbon-Carbon generated non-uniform surface temperature distributions. Further investigation using ANSYS workbench has shown that non-uniform temperature profiles can be created and controlled by modifying the total Joule energy supplied and geometry configuration of Reinforced Carbon-Carbon model. Final non-uniform temperature distributions were influenced by the shape, power supplied and the heat loss mechanisms present in a resistively heated object. Conclusions and recommendations for future use of resistive heating methods were made.

Contents

I.	Introduction	3
II.	Background and Motivations	3
	A. Previous work	3
III.	Project Overview	4
IV.	Material Selection	4
V.	Analytical Modeling	
	A. Resistive heating	5
	B. Radiation	5
	C. Natural convection	6
	D. Total Energy Transfer	7
	E. Justification Against Experimental Results	7
VI.	Finite Element Modeling Method	
	A. ANSYS Modeling Setup Conditions	8
	B. Electric Analysis	8
	C. Transient-Thermal Analysis	8
	D. Uniform Cross Sectional Area Results	8
VII.	2D Geometric Variation	
	A. Setup Conditions	9
	B. Results and Discussion	9
VIII.	Radiation and Convection Heat Loss Effects	
	A. Setup Conditions	9
	B. Results and Discussion	10
IX.	3D Geometric Variation	
	A. Setup Conditions	10
	B. Results and Discussion	10
X.	3D Geometric Variation	
	A. Setup Conditions	11
	B. Results and Discussion	11
XI.	Conclusions	12
XII.	Recommendations	12

¹ PLTOFF, School of Engineering & Information Technology. ZEIT4501

Acknowledgements	13
References	13

APPENDICES	
Appendix A. Numerical Calculation	A1

Nomenclature

V	=	<i>Voltage</i>
I	=	<i>Current</i>
R	=	<i>Resistance</i>
P	=	<i>Power</i>
A_{cross}	=	<i>Cross sectional area</i>
ρ	=	<i>Resistivity</i>
L	=	<i>Object length</i>
$A_{s,tot}$	=	<i>Total object surface area</i>
A_s	=	<i>Local surface area</i>
σ	=	<i>Stefan–Boltzmann constant</i>
ϵ	=	<i>Emissivity</i>
T_w	=	<i>Object wall temperature</i>
T_a	=	<i>Ambient temperature</i>
h	=	<i>Heat transfer coefficient</i>
Q_{tot}	=	<i>Total rate of heat transfer</i>
Q_{rad}	=	<i>Heat transfer through radiation</i>
Q_{conv}	=	<i>Heat transfer through Convection</i>
TDLAS	=	<i>Tunable diode laser absorption spectroscopy</i>
Pr	=	<i>Prandtl number</i>
Gr	=	<i>Grashof number</i>
Ra	=	<i>Rayleigh number</i>
Nu	=	<i>Nusselt number</i>
CMC	=	<i>Ceramic matrix composite</i>
RCC	=	<i>Reinforced carbon-carbon</i>
C/SiC	=	<i>Carbon reinforced silicide carbide</i>
2D	=	<i>Two dimensional</i>
3D	=	<i>Three dimensional</i>

I. Introduction

With continuing advancements in aerospace applications, systems are becoming more complex to analyse. There is an increasing need for greater accuracy in the simulation of flight conditions that aircraft systems are exposed to whilst in operation. One of these conditions is the non-uniform aerodynamic heating hypersonic vehicles are exposed to when they fly at high Mach numbers. The aim of this project was to assess the feasibility of maintaining non-uniform temperature profiles through resistive heating of a piece of RCC (Reinforced Carbon-Carbon) in both a steady state and transient condition. This was achieved by varying the distribution of energy through a piece of RCC throughout its shape.

The reasoning behind the selection of RCC as the reference material for this project was based off previous work done in this area, as well as the materials availability and desirable characteristics it possesses to be used in resistive heating applications. An example in which RCC material has been used in the past because of its favorable heating properties is on the leading edges and nosecone on the Orbital space shuttle. Upon re-entry, these areas of the shuttle were exposed to extreme heating. Using RCC paneling meant that the shuttle had the ability to withstand large heat loads and protect the structural integrity of the vehicle.^[1]

This purpose of this project was to investigate different ways in which resistive heating that could induce non uniform temperature distributions across the surfaces of different RCC geometries. These resistive heating methods analysed in this project could then be adapted to experimentation to map the non-uniform temperature distributions that different aircraft and their components are exposed to during operation.

II. Background and Motivation

This project was an evolution of previous experimentation where a piece of RCC was electrified to simulate the wall temperature conditions of a hypersonic vehicle. These changes in wall temperature profiles were a result of aero-thermal heat generated by high Mach numbers. The non-uniformity of these temperature profiles were made evident through the post-flight analysis of the USAF/DSTO's HIFiRE-0 mission. A component of this hypersonic flight test program involved coating the stainless steel nose cone on the vehicle with permanent-change thermal paints. The visible colour change on these permanent-change thermal paints indicated that the system during its test flight was exposed to heating and as a result generated a non-uniform temperature profile reading. From this test, resistive heating of RCC was as a method to experimentally simulate the wall temperatures the vehicle would have been exposed to. These simulated wall temperatures were then used to assess the thermal-structural characteristics of the TDLAS (*Tunable diode laser absorption spectroscopy*) system used in the USAF/DSTO's HIFiRE-0 mission.^[2]

In hypersonic conditions, surface heating occurs from compression as a result of shockwaves in the stagnation region and in viscous boundary layer heating.^[3] During the experiment, non-uniform temperature profiles were not replicated as the main focus of the experiment was to assess the thermal-structural characteristics of an optical component (Sapphire window) using within the TDLAS system. The experiment did demonstrate the potential of using CMCs (Ceramic Matrix Composites) to replicate inflight surface temperatures through resistive heating. Throughout the experiment, the temperature readings of both the CMC and the Sapphire window were measured using an IR camera. Temperature readings that were taken throughout the experiment indicated that there was a uniform temperature distribution throughout the CMC, and a non-uniform distribution throughout the sapphire window. This can be seen in Fig 1. The heating that occurred throughout the sapphire window was a resultant of conductive heat transfer from the Joule heat energy applied to the CMC. It is this conductive heat transfer that generates a non-uniform temperature profile across the surface of the sapphire window.

Other previous work where the resistive heating of RCC was used was in a method of calibration for permanent-change thermal paints.^[4] The method induced a transient thermal loading to generate different temperatures. To induce these transient conditions, a piece of RCC was resistively heated by controlling the amount of current passed through it. Rather than applying a current instantaneously the piece of RCC, the current applied was increased over time to ensure that gradual transient thermal conditions occurred. The rate at which this current was applied can be seen in Fig 2.

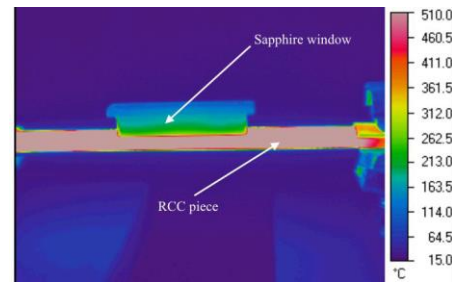


Figure 1. Hypersonic flight conditions simulation^[2]

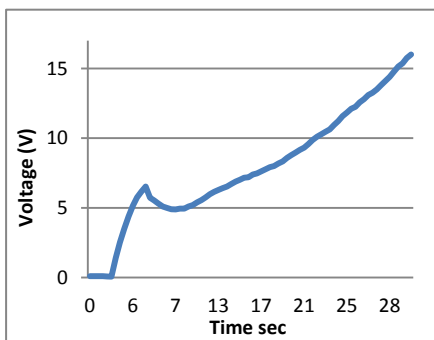


Figure 2. Voltage applied over time^[4]

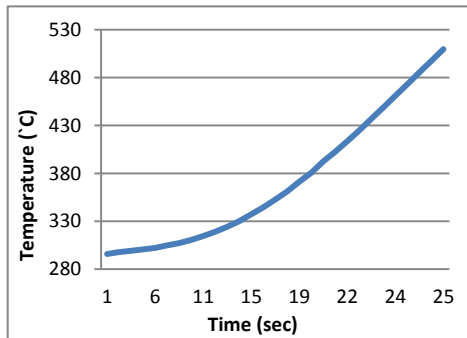


Figure 3. Temperature recordings from IR camera ^[4]
silicon carbide matrix.

The resultant surface temperature recordings were achieved using an IR camera and can be seen in Fig 3. The graphs indicate that when more current was applied to the piece of RCC, the temperature on the materials surface increased. The results from this experiment were used as a baseline for the numerical solutions calculated in this project.

The assumption throughout the majority of this project was that the material used in this experiment was RCC. Towards the end of this project, it was discovered to not be RCC but a similar CMC being C/SiC (Carbon Reinforced Silicide Carbide).

Even though RCC and C/SiC are different materials, their properties are relatively similar in relation to resistive heating. The difference being that RCC has a carbon matrix, whereas C/SiC is a

III. Project Overview

The aim of this project was to assess the feasibility of using Joule heating on an object made from RCC with varying geometry to generate non-uniform surface temperature profiles. This was achieved by deriving the numerical solution for surface wall temperature and analyzing the solution against previous experimental data. Using the program ANSYS, Finite Element Modeling was used to analyse the effect geometry variation has on generating non-uniform surface temperature profiles. Further investigation was conducted to assess the limitations of using Joule heating methods by analysing changes in the amount of electrical power provided and assessing how complex geometries affect progressive and final temperature distributions.

IV. Material Selection

Due to the assumption made in previous experimentation, RCC material properties were used throughout this project. The reason why RCC was initially considered within the realm of these applications was due to its desirable material properties for the purposes of resistive heating.

RCC is a manufactured composite, because of this there is a variation in its recorded material properties due to differences in manufacturing methods. RCC is constructed out of layers of carbon fiber sheeting encased in a matrix of carbon. Variability in material properties can occur from the changes in the orientation of the carbon fiber layers, the ratio of the carbon fiber layers to carbon matrix and the heating/cooling processes in the materials construction. ^[5] For the purposes of this project, a specific RCC material type was selected for consistency throughout the FEM (Finite Element Modeling) analysis. The material type model number of the RCC selected is 1001 G which is manufactured by the composite company @Sigrabon. ^[3] The main reason for this material selection was because it had published data for all the material properties required to complete numerical and computational analysis needed for this project.

To create temperature profiles on the surface of objects through resistive heating, the material must be electrically conductive. Electrical conductivity of a material is determined by the amount of resistivity that material has. When an object is resistively heated, it is preferable for the resistance to be low enough to hold a current and high enough to produce heat. RCC is favorable compared to other material as it is a nice compromise between being a good enough conductor to hold a current and a good insulator to not over heat.

Like all materials, properties of RCC will change with temperature. RCC is preferable over other materials as the changes in its materials properties are relatively small in comparison to other materials. During experimentation where resistive heating could be used to reproduce temperature profiles of flight conditions, a lower change in resistance means fewer changes would be required to the electrical power settings applied to that material to generate a desired thermal distribution.

When using the resistive heating method in experimentation, it is important that the geometry of the object is maintained as much as possible. For this to occur, it is preferable to have a material with a low coefficient of thermal expansion. RCC is a ceramic material that has a considerably lower coefficient of thermal expansion. The coefficient of thermal expansion for RCC-1001 G can be seen in Fig 4. The reason why there are two different coefficients of thermal expansion for RCC is because of the carbon fiber layering or sheets throughout the material. Expansion perpendicular to the carbon fiber layers is greater than

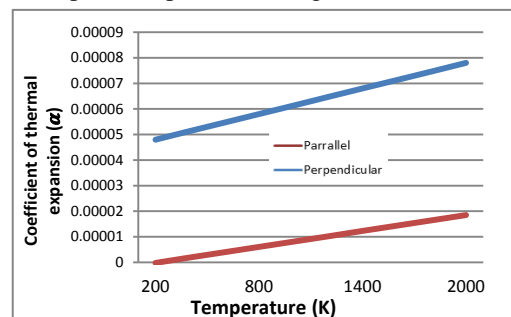


Figure 4. Coefficient of thermal expansion of RCC ^[5]

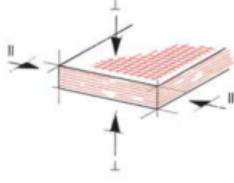


Figure 5. Typical construction of RCC [5]

it is parallel because the carbon matrix holding the layer together will expand more with heat than the carbon fiber layers. The coefficient of thermal expansion is lower in the carbon fiber sheets because it is made up of many small pieces of carbon woven together, compared to the carbon matrix where it has the internal bonding characteristic of one piece of carbon. An example of the construction of

RCC can be seen in Fig 5.

The orientation of RCC's carbon fiber layers also has an effect on the thermal conductivity of the object which can be seen in Fig 6. The graph also shows that changes in total thermal conductivity are more dependent on the thermal conductivity through the carbon fibre layers, rather than through the carbon matrix. A high thermal conductivity would be more desirable in a material if the intended surface temperature distribution is constant. Since the intention project is to develop methods for generating non-uniform temperature profiles, it would be more desirable to resistively heat a material with a lower thermal conductivity. A lower thermal conductivity means the temperature at a given point on an object will be more dependent on its electrical resistance, rather than having the heat energy conductively dissipated throughout the material.

Resistive heating of an object over a period of time can have the potential to induce thermal shock which occurs when a material exposed to sudden changes in its temperature. To avoid thermal shock a material must have a lower coefficient of thermal expansion, a high thermal conductivity, high yield strength and high fracture toughness, all of these being characteristics that RCC possesses. Thermal shock can also be easily avoided if the right processes are used when resistively heating RCC. Rather than applying a strong current straight away on the material, ramp up the power supplied to the material to allow surface temperature changes to occur over a period of time, rather than suddenly.

Resistive heating also relies heavily on the dielectric strength of a material which is the ability of a material hold a current without breaking down in structure.^[6] It is this ability that separates RCC from other ceramic composites. A greater dielectric strength means that more current is allowed to pass through a material, the higher the temperatures that can be reached for desired surface temperature distributions.

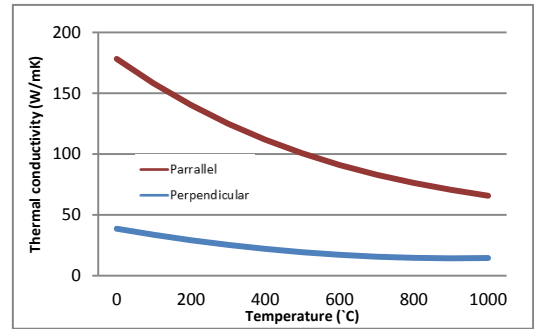


Figure 6. Thermal conductivity of RCC [5]

V. Analytical modeling

A. Resistive Heating

The concept of the project is based around the process of Joule heating. Joule heating occurs in an object when an electric charge is applied and the electrons inside the object become excited. These excited electrons generate frictional forces between molecules within the material. The energy from these internal frictional forces generates heat which is then released through the surface of that object.^[7] The amount of heat energy released from the object is proportional to the amount of electrical energy power provided to the model. This can be seen in Equation 1 where the Joule heat energy rate of a system is proportional to the electric power supplied to the system.

$$Q_{Joule} \propto P = VI = I^2 R = V^2 / R \quad (1)$$

The premise of this project is that by varying the geometry of an object, you can vary the amount of energy that is released through its surfaces. If the amount of voltage or current supplied to a system remains constant throughout an object, the resistance of a given point is the variable that must be changed to induce a non-uniform surface temperature profile. The equation for the electrical resistance of an object can be seen in Equation 2.^[8]

$$R = \rho L / A_{cross} \quad (2)$$

By varying the cross sectional area throughout an object the resistance will change throughout the object. Energy can then be released non-uniformly throughout the surface of an object. This in turn is what generates non-uniform temperature distribution across these surfaces.

B. Radiation

When an object is resistively heated, it releases heat energy into its surroundings. The most heat loss of a resistively heated piece of RCC occurs through radiation. Radiation heat loss does not require a change in mass

or a medium to occur.^[9] It takes place in form of electromagnetic waves mainly in the infrared region which can be detected by using thermal cameras. The rate at which heat is lost through radiated heat transfer is mostly dependent on the difference in temperature between the surface of an object and its surrounding ambient conditions. This can be seen in the following Equation 3.^[10]

$$\dot{Q}_{rad} = A_{s_{tot}} \sigma \epsilon (T_w^4 - T_a^4) \quad (3)$$

RCC has quite favourable emissive properties for resistive heating. Equation 3 shows the importance of emissivity. Like most solid material, the emissivity of RCC will change with temperature. These favourable emissivity properties can be seen in Fig 8. Here it is shown that within the first 1600 K there is only ~12 % variation in emissivity of RCC. This is highly desirable over other materials during experimentation because it makes it easier to gain temperature readings for materials using equipment such as an IR camera. Consistent emissivity with temperature is also important when resistively heating to generate non-uniform temperature profiles. Non-uniform temperature distributions along the surface of a material will generate a non-uniform emissivity distribution. This will affect the amount of heat lost throughout the material making it harder to control the shape of the non-uniform temperature distribution. Fig 8 also shows that there is a dramatic change in the emissivity of RCC at ~1800 K. This means trying to generate temperatures past this point will begin to become harder because more energy would be required to overcome this change in emissivity. Because of this it is recommended that RCC not be used to generate wall temperatures of greater than 1800 K.

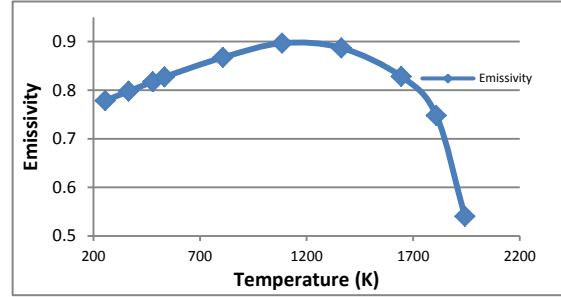


Figure 7. Emissivity change with temperature of RCC^[11]

C. Natural Convection

Convection heat loss of an object occurs when a moving fluid comes in contact with a surface of different temperature. The rate and which convection heat loss occurs can be seen in Equation 4.

$$\dot{Q} = hA_s(T_w - T_a) \quad (4)$$

The heat transfer coefficient in Equation 4 is used to quantify the effect the surrounding flow conditions in contact with the surface of an object has on the total convective heat loss.^[12] For this project, the assumption was made that the local conditions for experiments, numerical solutions and computational modeling of RCC took place in standard atmospheric conditions. This steady-state condition is known as a free vortex or natural convection.

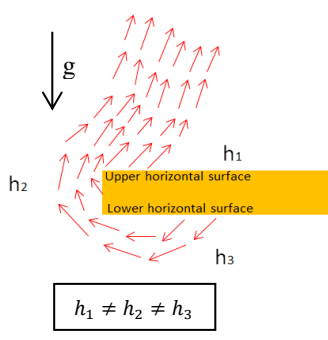


Figure 8. Natural convection rectangular prism

When a heated object is in natural convection conditions, the only influence on the fluid motion of the surrounding air is generated by the convective heat loss of that object. In this condition, the heat transfer coefficient of a surface is dependent on the orientation of that surface respective to level the Earth's surface (perpendicular to gravity. This involved analyzing three different surface orientations to calculate the heat transfer coefficients on a block of RCC. A visualization of natural convection can be seen on the Fig 8. The heated air from the object will interact with each surface differently, which generates a different heat transfer coefficient on each face.

The value of the heat transfer coefficient of a surface is dependent on the direction that surface is facing and its overall size. The heat transfer coefficients for both of the horizontal surfaces were found using Equation 5, and the heat transfer coefficients for the vertical surfaces were found using Equation 6.^[13]

$$h_H = Nu_H \frac{k}{(W \times L) / (2W + 2L)} \quad (5)$$

$$h_V = Nu_{V_{laminar}} \frac{k}{H} \quad (6)$$

To find the value for the Nusselt Number (Nu) for the horizontal upper surface, the following formulas were used.

$$Ra = Gr * Pr \quad (7)$$

$$Gr_{H_{up}} = \left[g\beta(T_w - T_a) \left(\frac{W*L}{2W+2L} \right)^3 \right] / \nu^2 \quad (8)$$

$$Nu_{H_{up}} = 0.54Ra^{0.25} \quad (9)$$

The same was applied to the horizontal lower surface

$$Gr_{H_{up}} = \left[g\beta(T_w - T_a) \left(\frac{W*L}{2W+2L} \right)^3 \right] / \nu^2 \quad (10)$$

$$Nu_{H_{down}} = 0.27Ra^{0.25} \quad (11)$$

and finally the vertical surface.

$$Gr_V = [g\beta(T_w - T_a)H^3] / \nu^2 \quad (12)$$

$$Nu_{V_{laminar}} = 0.68 + 0.67Ra^{0.25} / \left(1 + \left(\frac{0.492}{Ra} \right)^{\frac{9}{16}} \right)^{\frac{4}{9}} \quad (13)$$

All numerical calculations and computational simulations for this project were performed using the same sized block of presumed RCC in previously performed experiments with dimensions of 192 mm in length, 20 mm in width and 3.5 mm in height. Fig 9 shows how the heat transfer coefficients for each surface change with temperature. The greatest heat loss occurs on the vertical surface because as air is heated it will rise and new air will take its place. As the upper horizontal surface heats air, there is less opportunity for clean unheated air to replace the heated air and as such has a lower heat transfer coefficient. The total convective heat loss for this object can be seen in Equation 14.

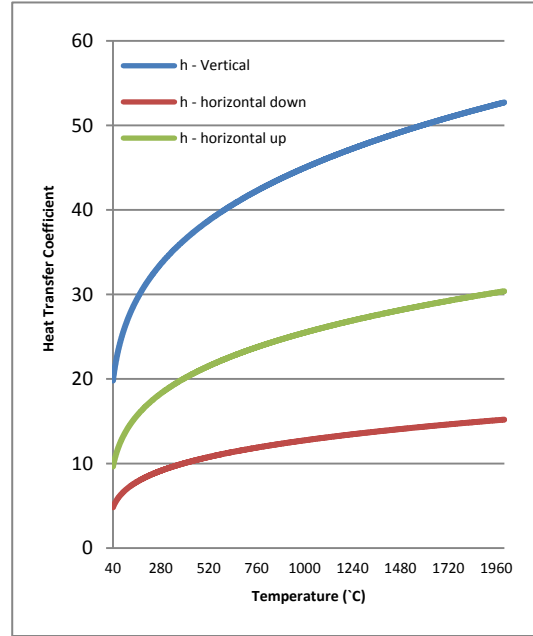


Figure 9. Heat transfer coefficient due to natural convection

$$Q_{conv.} = (h_1A_{s_1} + h_2A_{s_2} + h_3A_{s_3})(T_w - T_a) \quad (14)$$

D. Total energy transfer

For the purposes of this project, it was assumed that only idealized heat loss occurs when a piece of RCC is resistively heated. This means the total electric power supplied to the system is equal to the summation of the radiation and convection heat loss. The resultant formula was then used to numerically determine the wall temperature of against previously recorded experimental data.

$$\begin{aligned} \dot{Q}_{tot} &= P = \dot{Q}_{rad} + \dot{Q}_{conv.} \\ \rightarrow \frac{V^2 A_{cross}}{\rho L} &= A_{Stot} \sigma \epsilon (T_w^4 - T_a^4) + (h_1A_{s_1} + h_2A_{s_2} + h_3A_{s_3})(T_w - T_a) \end{aligned} \quad (15)$$

E. Justification against Experimental Results

When using the above formula to calculate the surface temperature of RCC against previously determined experimental data which can be seen in Fig 2 and Fig 3, the results do not line up. An example of this is when the data is analyzed at 25 second. At this point, 12 V is applied to the piece of RCC to produce a uniform surface temperature of ~511 °C. For the numerical calculation, all the property values were attained for a piece of RCC at 511°C. These values and the calculation can be seen in Annex A. The result from this numerical calculation shows that the wall temperature of the RCC piece showed that to reach temperature of 511°C in a steady state condition, the voltage applied would have to be closer to 2.1 V.

There are many contributing reasons for the inaccuracy of this result. The first one being having previously been mentioned is that the block of material experimented on is not RCC, but C/SiC. Both of these have similar properties to one another. But even though there may be similarities in these material properties between these two materials, the property values are not the same which is there is a considerable difference in the temperature readings.

The derived equation for wall temperature is mostly used when assuming a resistively heated piece of material is in a steady state. Meaning the heat energy release from the system is equal to the amount of input energy added to the system through Joule heating. In a real system, it will take time for an objects surface to

heat and reach this point. When the experiment was performed, the temperature readings of the piece of C/SiC were instantaneously measured as the applied current was gradually increased. This meant the applied current did not have enough time for the surface temperature reach stabilization.^[5]

In the experiment, further heat loss would have occurred through the clamps used to apply a current to the block of material. As the block of C/SiC was resistively heated, its temperature would have been considerable greater than that of the clamps. Since it had to be in contact with the block to apply current, conductive heat loss would have occurred from the C/SiC piece to the clamps. This discrepancy should have mostly been corrected for if the thermal image camera was calibrated correctly.

The voltage values that can be seen in Fig 3 were what were applied to the object. It would have been more beneficial for this project if the voltage readings were taken directly from the object as energy was applied.

Other sources of error could have been simple cases of experimental error. It is assumed that the experiment was conducted in steady STA conditions. If the environmental conditions were not controlled, further heat loss could have occurred through forced convection rather than natural convection and if the ambient conditions were not at STA, the final temperature readings would have been affected.

VI. Finite Element Modeling Method

A. ANSYS Modeling Setup Conditions

To prove that the numerical calculation could be used to find wall temperatures of RCC in idealized conditions, a computational model using ANSYS workbench was created. The temperature dependent material properties of RCC were then applied the models material in the engineering data.

The geometry imported into the simulation was a block of the same dimensions that was previously used in experimentation.

In order to find the wall temperature distribution of the resistively heated FEM models, two analysis components were used in the setup of each simulation; these analysis systems being an electric input function and transient thermal function. The function of the electric analysis is to resistively heat the block and assess the distribution of Joule heating energy. The transient thermal function then takes the solution from the electric analysis and used it to generate the wall temperature profiles on the surface of the each model. Fig 10 shows the setup of what can be seen on the user interface workbench screen to link the solution generated by the electric analysis to the transient-thermal analysis function.

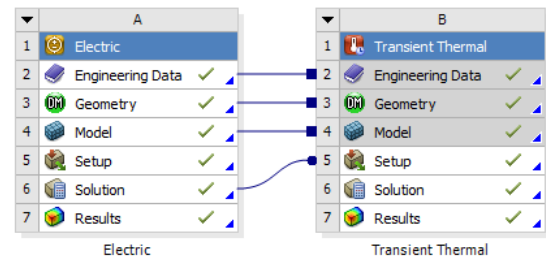


Figure 10. Link between electric analysis and transient-thermal analysis

B. Electric Analysis

For the purpose of proving the numerically derived equation can be used to determine wall temperature of an object at a steady state, a voltage difference of 12 V was applied across the length of each model. To ensure that the contact surfaces of where the voltage was applied did not interfere with the final wall temperature distributions on the surface of the block, a refinement was added during the meshing stages of this experiment. The remainder of the meshing consisted of a face sizing of 1mm on the top and bottom surfaces of the model.

C. Transient-Thermal Analysis

To acquire the temperature distribution for this model, the heat energy generated was imported from the electric model. Radiation and convection heat loss effects were then applied to the system in the setup of the simulation. The radiation effects applied were taken from the emissivity data in Fig 9 and the convection effects were taken from the heat transfer coefficient data in Fig 11.

D. Uniform Cross Sectional Area Results

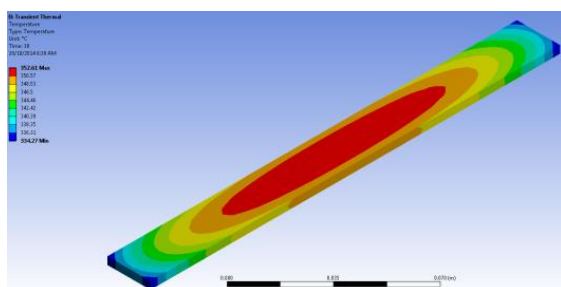


Figure 11. Link between Electric analysis and transient-thermal analysis

The results of this simulation shows what was supposed to be a uniform temperature distribution due to its constant cross sectional area along the length of the model ended up being non-uniform temperature distribution across the entire surface of the model. The reason why this occurred is due the radiation and convections heat loss conditions applied in the transient-thermal analysis input conditions. These conditions had to be added to the simulation so it could be comparable to the solution that would be found using the wall

temperature distribution equation. The FEM solution determined that when 12 V was applied across the length of the RCC model, the wall temperatures produced on the objects surface range from 331-354°C. When the material properties of RCC at 341°C (the average wall temp on the model surface distribution) were substituted into the numerical calculation the wall temperature solution was determined to be 348.2°C which falls within the range the simulated wall temperatures. This demonstrates the level of accuracy that can be achieved when using ANSYS to model temperature profiles induced by resistive heating.

VII. Geometric Variation

A. Setup Conditions

The purpose of these simulations was to assess the effect that 2D geometric variation has on surface temperature profiles. The simulations used the same set up conditions used for the uniform temperature profile simulation, except this time using four different imported models each with a different geometry. The construction of these consisted of a block of the same dimension as the previously performed experiment, except this time with a groove cut centrally located across the width of the material. This groove cut was to change the cross sectional area throughout the model to vary the resistance throughout the material. For each simulation model, the minimum cross sectional area exposed in the current flow direction was decreased by 10 mm².

The simulation was run with a voltage input of 4V instead of the previous 12V to ensure that the energy saturations effects of the material were limited. These effects were investigated further throughout the project.

B. Results and Discussion

The results in Fig 12 show the distribution of the temperatures recorded along the center path of length the RCC different models. As predicted, the point where the temperature readings of the simulation were the greatest was when the cross sectional area of the model is the smallest. It is also evident in the graph that as the minimum cross sectional area exposed to the current flow was decreased, the maximum temperature achieved was increased. This this relates back to the equation for resistance in Equation 2.

Further analysis of the graph also shows that the temperature profiles of the graph match the geometries made by different sized groove cuts. As each diameter in every groove cut was increased, the point at which the change in cross sectional area began was at a different point.

Another observation of the graph is when the minimum cross sectional area of the model was decreased, the maximum temperature increases, but the minimum temperature for that specific geometry model was decreased. The reason for this is because of the change in thermal conductivity of RCC with temperature. As the temperature of the model increases, the overall thermal conductivity of the model will decrease. As a result of this change, the temperature gradients of the material have increased around the points where the changes in cross sectional area begin to occur. This also leads into why the minimum temperatures of the models will decrease as their respective maximum temperatures will increase.

As cross sectional area decreases, the total resistance of a model has increased, which in turn increases the amount of power supplied to the model. The main contributing factor to the power that is applied to an object is the current. This related back to Equation 1 where the both current and voltage are squared in the power equation. This means that there is a change in the total Joule heating energy of a model. But this change is quite small when there is a small amount of geometric variation throughout a model. Since there is more energy concentrated at the points where cross sectional area of the model is decreased, less energy is distributed throughout the rest of the length of the model. Less energy release at a larger cross sectional area means a lower recorded surface temperature. This means that the higher the maximum temperature, the lower the minimum temperature.

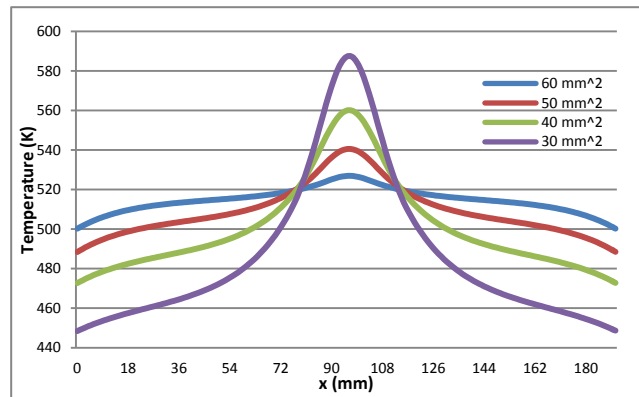


Figure 12. Lengthways temperature distributions of RCC with changes in minimum cross sectional area

VIII. Radiation and Convection Heat Loss Effects

A. Setup Conditions

The purpose of these simulations was to computationally assess the effects radiation and convection on a RCC model with geometry of inconsistent cross sectional area. The geometry used of these simulations was the

model used in the previous simulations with a minimum cross section of 40 mm² cross the midpoint of the length of the model.

Four different simulations were completed:

- Both radiation and convection applied
- Radiation applied, convection suppressed
- Radiation suppressed, convection applied
- Both radiation and convection suppressed.

Again, only 4V was applied through the simulation to avoid energy saturation.

B. Results and Discussion

Fig 13 shows the distribution of the maximum temperatures achieved over time for all of the simulated model conditions. It is evident the largest contributing factor to heat loss when RCC is resistively heated occurs through radiation heat loss. It can also be seen in the graph that the maximum temperature reached when only radiation is applied to the model converges at a steady state faster than it does when only radiation is applied. The reason for this massive difference can be seen in the equation for wall temperature.

The radiative heat loss is mostly dependent on the difference between the wall surface temperature and surrounding air temperature. Alternatively, heat loss through convection is more dependent on the value of the heat transfer coefficients, which they themselves are dependent on movement of the surrounding air flow. If this method were to be applied to systems that are exposed to a free vortex, the amount of heat loss through convection would be increased.

The model also shows that if there are no heat loss mechanisms in the system, the maximum temperature of the model will continue to increase and will never reach a steady state.

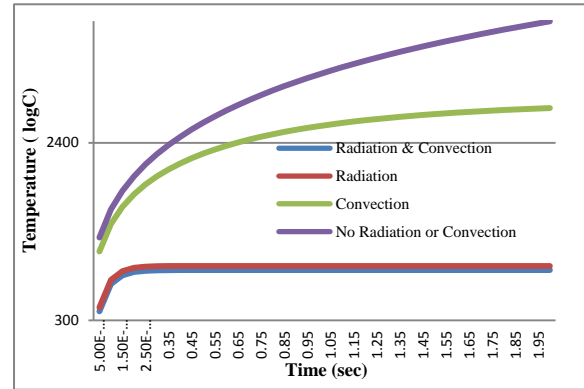


Figure 13. Wall temperature distributions of varying heat loss systems

IX. 3D Joule Heating Effects

A. Set Up Conditions

The purpose of these simulations was to assess the effect that 3D geometric variation has on surface temperature distributions. The simulations in this stage of analysis used the same set up conditions used for the uniform temperature profile simulation except this time using different imported geometries. Six different import geometries were constructed in CATIA, each with a spherical groove cut made in the centre of the lower surface of the block. Each of the groove cuts has a radius of 9 mm and with minimum thicknesses from 0.5 mm to 3.0 mm. A voltage of 10V was applied to the models during all simulations.

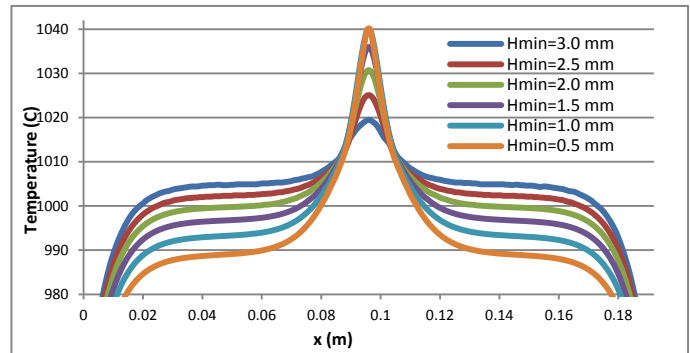


Figure 14. Midpoint heat distribution along block length

B. Results and Analysis

The results in Fig 14 indicate that along the length through the centre of a material, the resultant temperature distributions behave in the same way that it did during two-dimensional (2D) analysis. On closer inspection of the figure, it can be seen that all the temperature profiles intersect one another at the same points. These points being the start and finish of the changes in cross sectional area. The reason why this occurs at these points is because the changes local electrical resistance of the model starts and finishes at these points.

The way in which thermal distribution of geometries varies in three dimensions compared to two can be seen in Fig 15. At smaller cross sectional areas, the temperature distribution behaviors in the way as it did in 2D analysis. But as this thickness was

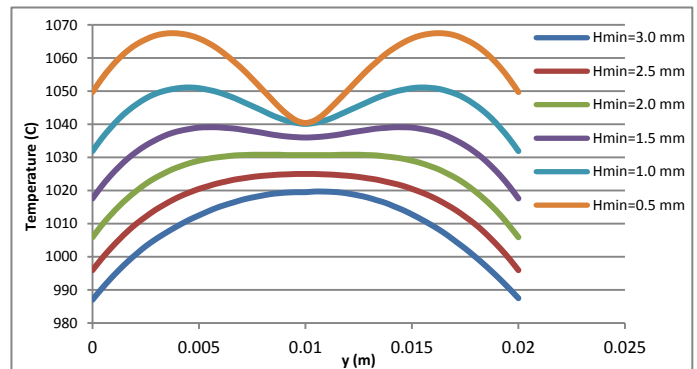


Figure 15. Midpoint heat distribution along block width

decreased, the temperature at the centre of the upper surface began to no longer be the maximum temperature.

As groove depth increases, the amount of heat energy the centre thickness of a model is able to maintain reaches a maximum. Once it begins to reach this maximum Joule energy loading, the heat energy will conductively dissipate throughout the variation in cross sectional area.

X. Complex Geometries

A. Setup Conditions

The purpose of these simulations was to computationally assess the temperature distributions generated when a current is passed through geometry of complex configuration. The imported geometry used in these simulations was had three evenly spaced 2D grooves across its length. Two sets of simulations were then performed using this geometric configuration. The first was to determine how temperature distributions change over time and the second was to assess the change in temperature distributions when the voltage applied to the model was varied.

B. Results and Analysis

The results of the first set of complex geometry simulations behaved in the similar way to previously conducted simulations. Fig 16 shows how the minimum and maximum temperatures were increased over time until they both reached a point of stabilisation. The temperature distributions across the surface of the material reached a point of stabilisation when the Joule heat energy of the model is equal to the heat loss of the system. These results feed back into the reason why the instantaneous temperature readings that were taken during the permanent-change thermal paints calibration test would have been have been inaccurate. Resistively heated RCC takes time to reach a steady state. If there is a need to generate a non-uniform temperature profile along the surface of an object, it would prove to be more beneficial to have the voltage remain constant and applied for long enough until the desired temperature distributions are achieved.

The second stage of simulations conducted was to assess how changes in the power supplied to a model of RCC will affect its surface temperature distributions. It was already known that when more power supplied to a model, the greater the surface temperatures of that model. Rather than analysing the temperatures reached when the voltage applied to a system was changed, Fig 17 shows the percentage of the maximum temperature at point along the length of a model. Equation 16 was used to find the values of the y-axis in Fig 17.

$$y = 1 - \frac{T_{Max} - T_{local}}{T_{Max} - T_{Min}} \quad (16)$$

The amount of power supplied to the model of RCC has a large effect on the way in which temperature is distributed across the model. When smaller amounts of power are supplied to the system, as can be seen in Fig 17 when 2.5 V is applied, there is only enough energy for the minimum cross sectional area in the centre of the model to reach its maximum. This is due to the construction of the geometry. Even though the groove cuts are evenly made along the length of the material all with the same radius, when resistive heating is applied, the centre groove cut is exposed to thermal conductive heating effects from both groove cuts made either side of it. Alternatively, the outside groove cuts of the model are exposed to thermal conductive heating effects from the centre groove. Because of this, the minimum cross sectional area at the centre of the model will have a higher energy loading which generates a higher temperature.

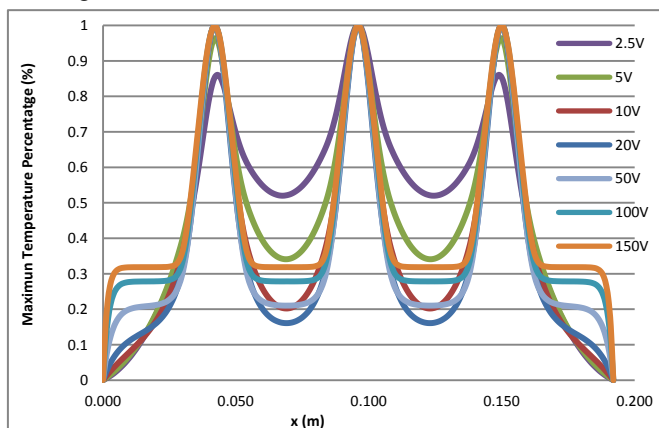


Figure 17. Voltage Variation in Complex Geometries

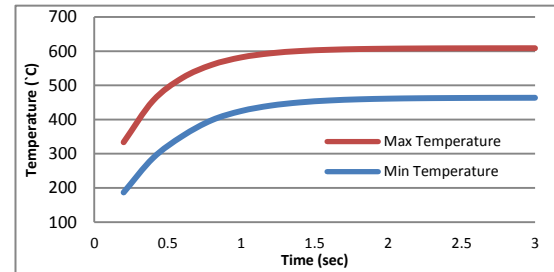


Figure 16. Temperature Change with Time for a Complex Geometry

When more power was applied to the model, the minimum cross sectional areas of each of the grooves reached the same temperature. This is because when too much energy is applied to a system, it will distribute that energy throughout the rest of the block through thermal conductivity. This is why Fig 17 shows that when more energy is added to a system, the temperatures along the length of the model, where cross sectional area is maximum and constant, will increase. The more energy added to a system, the harder that system will

work to stay in balance. This means that if the energy supplied to the model continued to be increased, the model would eventually reach a power input condition that would generate a constant temperature distribution.

XI. Conclusions

This project has shown non-uniform temperature distributions on the surface of RCC can be generated by varying the cross sectional area throughout an objects geometry. The shapes of these distributions were a function of the power supplied to the system, heat loss effects and the material properties. When using this method of thermal replication, if too much electric power is supplied to a system surface temperatures produced may exceed the material limit temperature. The material's natural reaction is dissipate this energy will interfere with the desired temperature distribution.

The extent to which this method of thermal mapping can be applied to experimental situations still requires further investigation. Even though geometric manipulation does produce non-uniform temperature profiles, controlling the shape of these temperature profiles could prove to be difficult in the future applications.

It has been observed that if greater temperatures are required on the surface of a RCC model, the most effective way to reach these temperatures is to increase the power supplied to the system. This will increase the overall Joule heat energy of the model, and will have a greater concentration of Joule heat energy as the cross sectional area perpendicular to the path of electric flow is decreased.

Controlling the shape of a temperature distribution of a model should be accomplished by governing the amount of geometric variation of a model and power supplied to the model. If a specific temperature is desired at a certain point on the surface of the model, it would be more beneficial to reach that designated temperature by varying the geometry of the object. Changes in the power supplied to a model have a greater effect on the final temperature of that model compared the effect of changes in cross sectional area. Changes in the geometry of a model will rearrange the already present Joule energy, whereas variation in the power supplied to the system (through current or voltage change) will change the total amount of Joule energy present in a model. In experimentation, more power is supplied to a system by increasing the amount of electricity applied to a model. This increases the risk to the members running the experiment. If the require power supplied to the model can be decreased, the overall safety of the experiment can be increased.

Alternatively, the disadvantage of controlling temperature in this way occurs when manipulating the geometry an object. For experiments where RCC has been chosen as the martial to be resistively heated, changes in the model geometry will be permanent and will have to occur prior to the experimental execution.

In an ideal experimental situation, the best way to generate desired surface temperature distributions of resistively heated RCC is to have a controllable electrical power source and a pre-determined material geometry. Decreases in the materials minimum cross sectional area and increases in the power supplied to an object not only generate higher maximum temperatures, but makes the changes in temperature along the surface of an object more pronounced.

XII. Recommendations

If investigations into this resistive heating method where to continue on in the future, it is recommended that a numerical comparison using the material properties of C/SiC be performed against the previously determined experimental data found in the calibration for thermal paints. By preforming these simulations, the results found in this project can be confirmed against real results.

Once this has been confirmed, the methods used in this project can be applied to other real world applications. Some of these would include assessing the thermal distributions across complex geometries. The model geometries used in this project are not an accurate representation of the shape of objects that are exposed to heating effects that produce non-uniform temperature distributions.

Once C/SiC has been proved against previously determined experimental results, further potential materials could be assessed to determine their usefulness in resistive heating applications. This project has assessed the usefulness of using CMCs as resistive heat generators for experimental applications. There are many other different materials that when resistively heated will produces a non-uniform temperature distribution across its surface. Observations of the material properties of RCC were made to justify it as an appropriate material for resistive heating. There is the potential for other materials to have to same justifications made for their specific resistive heat application.

An important future expansion of this project would be to access the affect that changes in the temperature of a material will have on the structural integrity. Non-uniform surface temperature distributions have the potential to create point of stress throughout a material. RCC was specifically selected because of its desirable thermal-structural properties. It would be important to justify these assumptions by analysing the transient structural conditions of RCC when it is resistively heated.

Acknowledgements

The author would like to acknowledge the guidance and support provided to him by his thesis supervisor A/Pro. Andrew J. Neely throughout the span of this project. The author would also like to thank MR. Rishabh Choudhury for providing knowledge and understanding on previous experiments and research conducted in this project area, Mr. Jai Vennik for providing critical assessment and advice throughout the critical stages of this project, and to the undergraduate peers also completing their final year project for providing essential feedback and motivation throughout this project.

References

¹National Aeronautics and Space Administration., “Carbon Fiber-Reinforced Carbon.” 2001 [Online] Available at: <http://www-pao.ksc.nasa.gov/kscpao/nasafact/pdf/RCCpanels-06.pdf>. [Accessed 21 October 14]

²Dasgupta, A., Rishabh, C., Neely, A., O’Byrne, S. and Kurtz, J. “Thermal-structural modelling of TDLAS system for SCRAMSPACE hypersonic flight test” *18th AIAA/3AF International Space Planes and Hypersonic Systems and Technologies Conference*, AAIA 2012-5900, Tours, France, 2012.

³Benson, T. (2014). *Compressible Aerodynamics*. Available: <http://www.grc.nasa.gov/WWW/k-12/airplane/bgc.html> Last accessed 1st Nov 2014.

⁴Rishabh, C. and Neely, A., “Calibration of Thermal Paints for Surface Temperature Measurement of HIFiRE-0 Flight” *18th AIAA/3AF International Space Planes and Hypersonic Systems and Technologies Conference*, AAIA 2012-5899, Tours, France, 2012.

⁵SGL Carbon Group, “Carbon Fiber-Reinforced Carbon – Properties and Uses.” 2004 [Online] Available at <http://edge.rit.edu/content/P07109/public/Design%20I/Published%20Research%20Document/CARBON%20FIBER%20PROPERTIES.pdf>. Last accessed 19 Oct 2014

⁶Elert, G. (1998). *Dielectrics*. Available: <http://physics.info/dielectrics/> . Last accessed 19 Oct 2014.

⁷help.autodesk.(2007). *JouleHeatingSetup*., Available: <http://help.autodesk.com/cloudhelp/2014/ITA/SimCFD/files/GUID-ED418E2B-26BD-4351-886A-E6C0AF8F1EF5.htm>. Last accessed 29th Nov 2014.

⁸Nave, R. (2005). *Resistivity Calculation*. Available: <http://hyperphysics.phy-astr.gsu.edu/hbase/electric/resis.html>. Last accessed 18 Oct 2014.

⁹EDinformatics. (1999). *How is Heat Transferred*. Available: http://www.engineeringtoolbox.com/radiation-heat-transfer-d_431.html. Last accessed 20 Oct 2014.

¹⁰Nave, R. (2005). *Heat Radiation*. Available: <http://hyperphysics.phy-astr.gsu.edu/hbase/thermo/stefan.html>. Last accessed 18 Oct 2014.

¹¹Ohlhorst, C., Vaughn, W., Lewis, R., Milhoan, J. and Koenig, J., “Emissivity Results On High Temperature Coatings for Refractory Composite Materials” 29th International Thermal Conductivity Conference (ITCC) and 17th International Expansion Symposium, Birmingham, AL, 2007

¹²Pamler, D. (2014). *Flow Profile Over a Flat Plate*. Available: <http://www.efunda.com/about/contact.cfm>. Last accessed 18 Oct 2014.

¹³Schlichting, H., *Boundary Layer Theory*, 7th ed., McGraw Hill Book Company, New York, 1979